TURBULENT JET NOISE CONTROL BY FLUID CHEVRONS

Estelle Laurendeau, Peter Jordan, Jean-Paul Bonnet and Joel Delville
Laboratoire d'Etudes Aérodynamiques,
UMR-CNRS 6609 - Université de Poitiers - ENSMA
CEAT, 43, route de l'aérodrome F-86036 Poitiers, FRANCE
estelle.laurendeau@lea.univ-poitiers.fr

ABSTRACT

The paper deals with an experimental study of a fluid control device for subsonic jet noise. The device comprises an azimuthal arrangement of secondary subscale jets (named *fluidevrons*) which mimic the well known chevron geometry. The advantage of this method is that the "geometry" can be adapted according to the motor regime, thus avoiding the thrust penalty during cruise for aircraft applications. In the low frequency range, the effect is to reduce the noise, typically for Strouhal numbers less than 3. For higher frequencies, the pressure levels observed are found to slightly increase. The aerodynamic and acoustic effect of the *fluidevrons* is examined in this work, and the consequent changes to the source mechanisms discussed.

BACKGROUND AND OBJECTIVES

A large number of studies on passive flow control devices have been conducted for jet noise reduction, leading to the current state-of-art technology of chevrons for medium and high by-pass turbofan engines. The modifications of the flow at the nozzle trailing edge has been shown to lead a reduction of the sound intensity produced by the jet. While the mechanism underlying the efficiency of the chevron is not entirely understood, it seems to lie in their ability to induce streamwise vorticity in the shear layer and to destroy the natural azimuthal modes. This paper deals with a concept which mimics the chevron concept through the generation of fluidic deltas by means of an azimuthal arrangement of secondary subscale jets. Hereafter named *fluidevrons*, these fluid chevrons allow a comparable effect in terms of noise reduction, with the advantage of being an on/off actuator.

The objective of this study is to better understand the physical mechanisms by which this device reduces the sound production capacity of the flow. Thus turbulent flow field is investigated using PIV and hot-wire measurements, and the observed trends are related to some preliminary acoustic measurements by means of both an acoustic analogy, and large structure model of the jet noise source mechanism.

THE EXPERIMENTAL SET-UP

Flow and nozzle configuration

The experiments were conducted on a single flow free air jet at $M = 0.3$. The boundary layer is tripped to assure it is turbulent at the exit plane. On a 50 mm diameter nozzle, we placed eight pairs of converging jets, each pair forming a 60^o angle in the azimuthal direction. They are inclined towards the main jet axis with an angle of 12^o. A view of the demonstrator is shown in figure 1. In terms of optimisation of the control jets, two internal diameters 0.86 mm and 1.5 mm were tested for different blowing rates $C_\mu = Q_{MJ}/Q_{TCJ}$ varying from 0.3% to 2% of the main jet mass flow where Q_{MJ} and Q_{TCJ} are respectively the micro-jets and the main jet mass flow. The optimum configuration is an internal diameter of 0.86 mm with $C_\mu = 1\%$ and jets exit velocity $V_{jets} = 208$ m.s^{-1}.

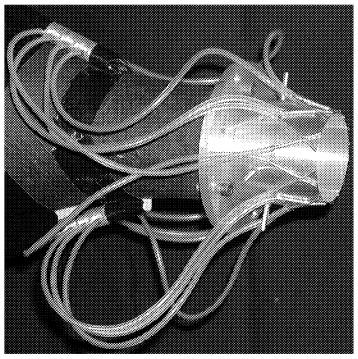

Figure 1: Device apparatus

MEASUREMENT TOOLS

Acoustic measurements

Quasi-far field acoustic measurements were performed with B&K microphones placed at 20 diameters from the jet axis for different angular positions. These are only preliminary results as they were effected in a laboratory environment without acoustic treatment.

PIV system and data processing

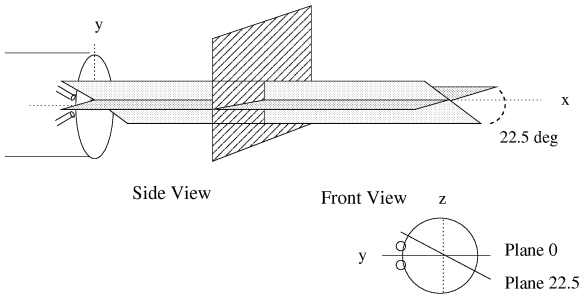

Figure 2: PIV planes

Acquisition system.

PIV data was acquired in planes normal to the jet axis, at four different axial locations allowing direct measurements of the cross-stream gradients and features induced by the device. Measurement at axial positions of $0.5D$ and $1D$ were used to provide details of the initial shear layer development and the local action of the *fluidevrons*, measurements at $3D$ and $5D$ being used to understand the global effect on the flow. Measurements were also performed in planes parallel to the jet axis (Fig.2) for two different azimuthal angles, in a plane containing the tip of the pair of jets (plane 0) and in a second plane falling between two pairs (plane 22.5).

The PIV system was implemented using two $1040 * 820$ acquisition cameras synchronized to a 300 mJ/pulse PIV ND-YAG laser. For measurements along the jet centerline, the laser sheet was parallel to the jet axis, with a pulse duration of $10ns$, whereas for cross-stream measurements, the laser sheet was normal to the jet axis, illuminating the cross-section with a pulse of 12 ns. For the image calibration we used a $200x200$ mm^2 grid target and the acquisition process was monitored by the Davis software v 6.2. For cross-section views a glass window was placed in front of the camera to protect it from the flow and the seeding. Two different camera apertures were used as a compromise between precision and the minimum distance between the nozzle and the glass window, so that the flow is not perturbed.

The jet flow was seeded using high density smoke fluid in a power mist close to the air inlet, with a re circulation plastic tunnel, large and wide enough to assure no perturbation of the flow. No seeding was implemented for the control jets, due to their small diameters. It was judged that this should not have a significant impact on the measurements as we did not come closer than $0.5D$ from the jet exit, which is beyond the end of the potential core of the control jets, estimated using the Lau *et al* formulation $L_{pc} = (4.2 + 1.1M_e^2)D$, i.e. less than 4 mm in the present configuration. For views in planes parallel to the jet axis, PIV measurements closer than 0.5 D from the jet axis are parasited from light reflections on the nozzle and therefore not considered in this study.

PIV processing and estimation of measurement errors.

The processing of the PIV views was effected using the Lavision software. The measurement accuracy depends mainly on bias errors related to two major factors: the seeding and the size of the interrogation window. Random errors are supposed here small considering an ensemble-average of 1000 vector fields.

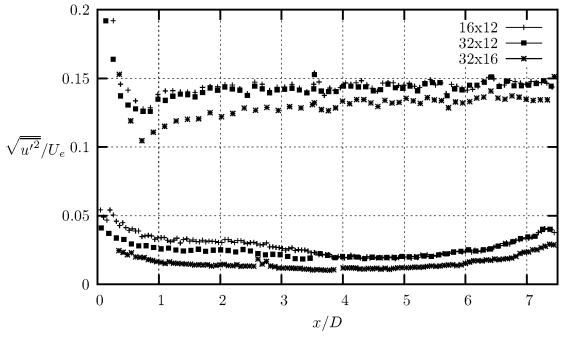

Figure 3: Influence of the interrogation window's size on the longitudinal component $\sqrt{u'^2}/U_e$ along the mixing layer axis ($y/D = 0.5$) and outside of the jet ($y/D = 1.5$) (plane 0, controlled case)

From the study of Christensen (2004), and the work of Westerweel (1997), the error associated with the sub-pixel estimator will be accentuated if the particle size is less than 1.5 pixels. For the size of the views in our configuration, the reflected diameter of the illuminated particles is of the order of one pixel. This makes the accuracy of the result sensitive to the size of the interrogation window and therefore a pre-study was effected in order to determine this effect.

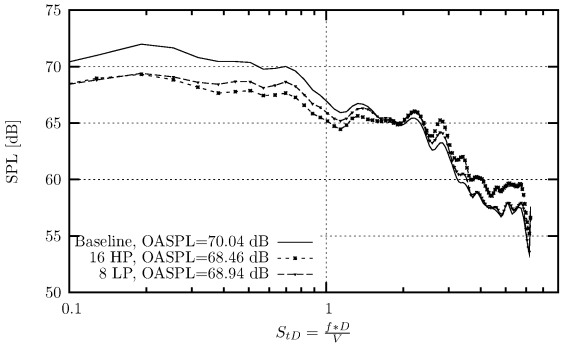

Figure 4: Two chevrons configurations spectra at $\theta = 90$, and 20 D from the jet exit

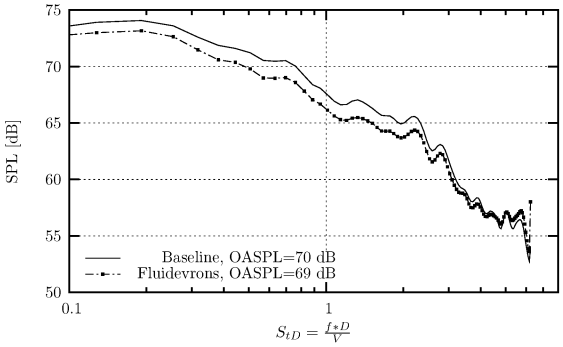

Figure 5: Effect of *fluidevrons* on spectra at $\theta = 90$, and 20 D from the jet exit

It was found that a multi-grid adaptive scheme comprising two estimations of the velocity field minimised the errors associated. For the mean values, results seem to be quite insensitive to the window size, as already seen by Christensen (2004). The effect becomes significant for the estimation of the fluctuating velocity components. As the window size decreases, the noise increases for measurements in the potential core. This effect is shown in figure 3. However, a smaller window produces better results in regions of high shear. The procedure adopted thus involved the use of two different grids: a $32x12$ adaptive multi-grid scheme for the mixing layer region where gradients are high, and a $32x16$ adaptative multi-grid elsewhere, resulting in two domains. The same procedure is used for the baseline and the controlled cases.

RESULTS AND DISCUSSION

An acoustic comparison between chevrons and *fluidevrons*

In order to compare the performance of this new control device with the classical chevron geometry, acoustic measurements were performed on a 16 chevron nozzle with two levels of penetration, $1/2\delta$ and 2δ, as well as a particular type of nozzle with 8 chevrons likewise one chevron out of two, with a baseline of 16 chevrons. Figure 4 shows the sound pressure level ($fe = 50{,}000$ kHz) of a 90^o spectrum in terms of the Strouhal number for two configurations: 16 high penetration chevrons (16 HP) and 8 chevrons with a nominal penetration (8 LP). These spectra show the impact of the nozzle configuration away from the peak

Table 1: Summary of nozzle geometry

Nozzle	Number of chevrons	Penetration
Baseline	0	None
16 HP	16	2 δ
8 LP	8	δ

emission direction. The results in configuration 1 show a decrease in the low frequencies of about 3 decibels and an increase in the higher frequencies, with an inversion point at a Strouhal number of 2. These results exhibit trends similar to those obtained by Bridges (2002).

Figure 5 shows the effect of *fluidevrons* under the same conditions. The effect in terms of the noise radiation is to reduce the low frequency noise by about 2 dB, while increasing the high frequency noise. Thus, the usual trade-off between gain and loss is found as with the chevrons. However, the inversion point is shift to higher frequencies at a Strouhal number of 4.5. The effect of the *fluidevrons* would appear to be more subtle than the chevron effect, with less noise produced by the local effect of the device.

Aerodynamic results from PIV measurements

The global aerodynamic changes induced by the *fluidevrons* are here examined, with a view to better understand the underlying mechanisms and their subsequent impact on the sound field produced by the jet. Two main regions can be identified. The first is found close to the jet exit, where a local effect of the *fluidevrons* is manifest. It will be seen how the changes to the flow structure in this region can be associated with the penalty induced by control, i.e. the increased sound production at high frequency. The changes in the second region on the other hand, situated downstream of $x/D = 2$, can be considered as the global influence of the control mechanism, and as we shall see are responsible for the noise reduction in the energy containing spectral regime.

The changes to the local flow field can be appreciated through examination of the mean velocity vectors plotted in figure 6. This figure obtained from PIV shows a cross-section of half of the jet at $x/D = 0.5$. The local changes to the flow field are interesting, comprising a number of effects. It can firstly be noted how two pairs of counter-rotating longitudinal vortices are generated, one on the the low speed side of the mixing-layer, the other on the high speed side. These will be instrumental in inhibiting the development of the spanwise vortical structures more natural to a round jet, and so important in controlling the mixing rate and the global characteristics of the flow. It can furthermore be seen how the flow field appears to have been divided, on account of the said vortex pairs, fluid being both ejected from and entrained into the high speed region of the flow. The signature of this field can be seen in the radial profiles of the mean axial and radial velocities at $x/D = 0.5$ shown in figure 7. It can be seen how there is an initial expansion of the mean flow field, manifest in the mean axial velocity profiles. This expansion is of course due to the increased mixing just discussed. Not surprisingly, the fluctuating components of the velocity field are increased in this region of local influence. This can be seen in figure 9 which shows profiles of $\sqrt{\overline{u'^2}}/U_e$ and $\sqrt{\overline{v'^2}}/U_e$ at $x/D = 1$. It is also interesting to note that the *RMS* levels in the potential core have also been increased close to the jet exit (Fig. 9). This is likely a result of the increased local entrainment due to the counter rotating vortices on the high-speed side of the mixing layer, as discussed earlier.

The global effect of the *fluidevrons* is now discussed. The axial evolution of the mean axial velocity, shown in figure 8 demonstrates how the *fluidevrons* have caused an increase in the length of the potential

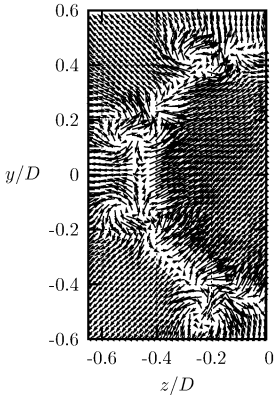

Figure 6: Vortical area created in between two microjets, $x/D = 0.5$

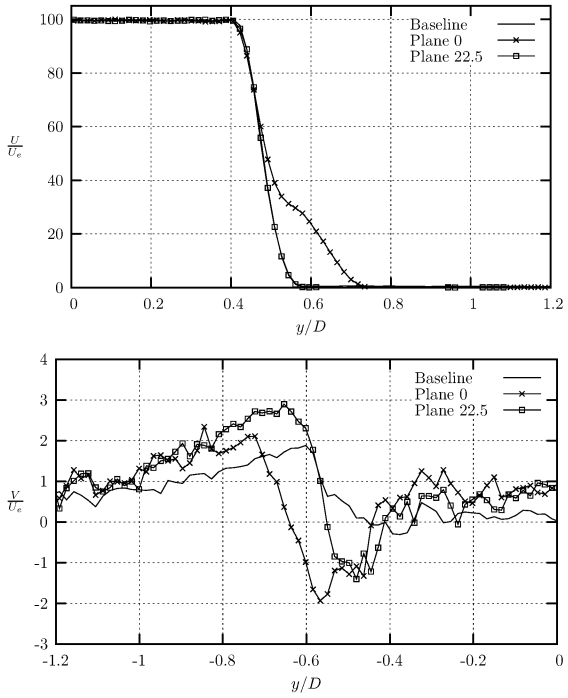

Figure 7: Mean axial and radial velocity profiles at $x/D = 0.5$

core of the order of 10%, and a corresponding decrease in the expansion of the flow field shown in table 2. We see thus how the global effect of this device is to decrease the mixing efficiency of the flow. Turbulence levels are reduced by more than 10% for the three components with a maximum of 15% reduction for the radial fluctuating velocity found for $x/D = 3$ (shown in figures 10 and 11). The probable cause, already alluded to, is a disruption of the development of the kind of azimuthal vortical structures preferred by the jet. The spanwise vortical motion characteristic of these structures is an efficient exchange mechanism between the potential core flow and the surrounding ambient fluid. The azimuthal action of the fluidevron pairs will inhibit the generation of these azimuthal structures in the intial stages of the flow's development. So the global effect is comprised by a mixing layer with reduced turbulence levels, a reduced expansion and a longer potential core.

Changes to the source mechanisms

To understand the effect which these changes to the aerodynamic

Table 2: Mixing layer's caracteristics

Variables	Baseline	Plane 0.	Plane 22.5
$(x0, y0)$	-0.25,-24.02	-0.88,-24.64	-0.67,-24.66
$d\delta_\omega/dx$	0.124	0.112	0.112
	region 1: 0.117	0.110	0.110
	region 2: 0.123	0.109	0.105

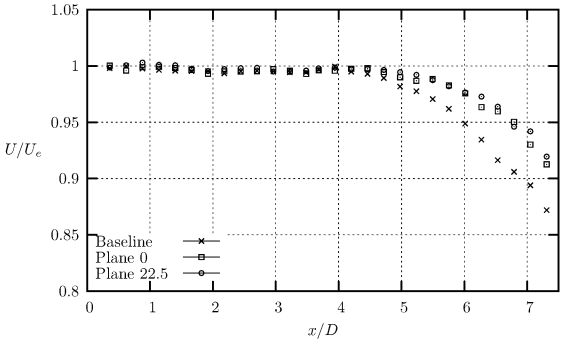

Figure 8: Centerline longitudinal velocity decay

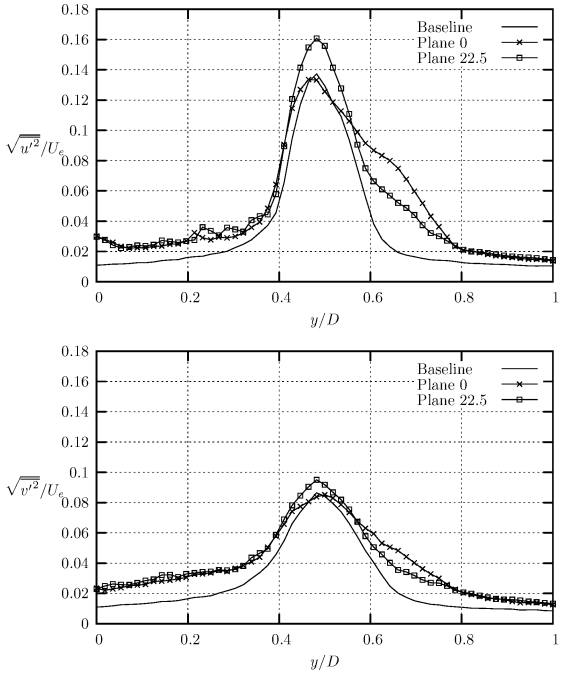

Figure 9: Fluctuating axial and radial velocity profiles at $x/D = 1$ (two different grids)

structure will have on the sound production mechanisms comprised by a free jet we must look to the different analytical and phenomenological descriptions frequently used for these. The existence of two kinds of source mechanism is commonly accepted. The first is related to the large structures of the flow, radiation from which is considered to be most important at angles close to the jet axis. The behaviour of this source mechanism is synonymous with the dynamics of the coherent azimuthal structures (see Guj *et al.* (2003), Hileman *et al.* (2004) and Jordan *et al.* (2003) for example). Their dynamic upstream of the end

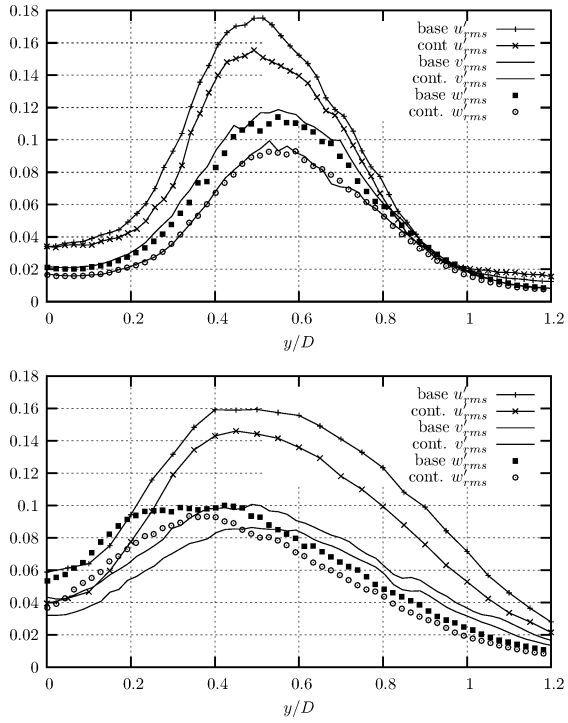

Figure 10: Fluctuating axial, radial and transversal velocity profiles, at $x/D = 3$ and $x/D = 5$

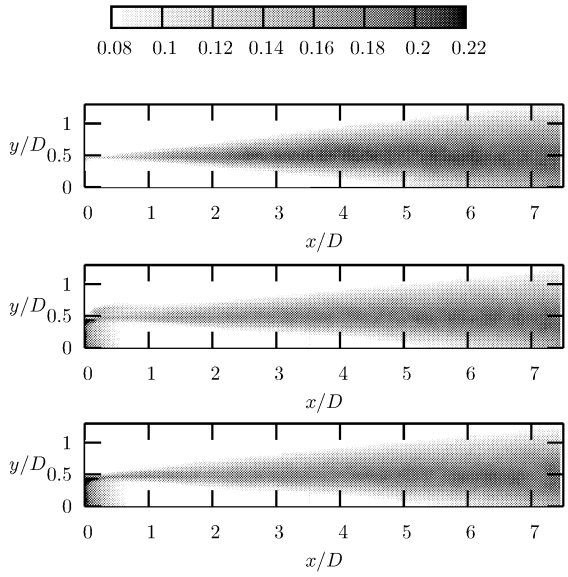

Figure 11: Influence of the control on the TKE, from top to bottom: baseline, plane 0 and plane 22.5

of the potential core radiates a coherent sound field, identified by Jordan *et al.* (2003), and their collapse just downstream of the same has been identified by Hileman *et al.* as a major source of high energy sound producing events. The inhibition by the *fluidevrons* of the development of the preferred coherent azimuthal structures of the jet, discussed earlier, is thus clearly going to reduce the efficiency of this particular source mechanism, both in its action upstream and downstream of the end of the potential core. The second source mechanism is related rather to the

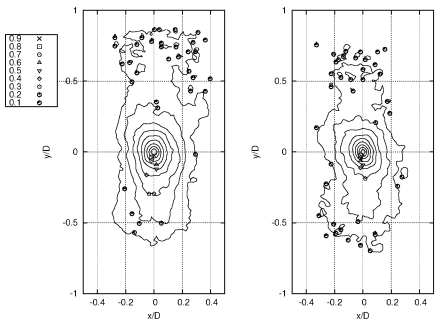

Table 3: Contours of the correlation coefficient $R_{vv'}$ on the mixing layer axis at $x/D = 4.5$ for the baseline (left) and the controlled case (right)

small-scale turbulence, and in order to appreciate the turbulence quantities implicated in this mechanism we must have recourse to the farfield solution of Lighthill's acoustic analogy (see Lighthill (1952) for details), given by equation 1.

$$P(y,\theta) = \frac{\rho_0}{16\pi^2 c_0{}^5 x^2 C^5} \quad \frac{x_i x_j x_k x_l}{x^4} \quad \int \frac{\partial^4}{\partial \tau^4} \overline{u_i u_j u_k{}^* u_l{}^*} d^3 r \qquad (1)$$

The intensity of a sound field produced by an unbounded turbulence which can be represented by an uncorrelated distribution of acoustically compact convected quadrupoles, as represented by the said equation, is seen to be related to the volume integral of the fourth time derivative of the fourth order velocity correlation tensor. The quantities implicated in the generation of sound according to this source model are thus (*I*) the Reynolds stresses, which appear in the said tensor, (*II*) the spatial extent of their correlation, which will be central in determining the value obtained from the volume integral, (*III*) the time scale characteristic of the temporal part of the correlation, which will contribute both to the spectral character of the sound field (via four temporal differentiations), and the amplitude of the sound field - smaller scales being representative of higher accelerations and efficient unsteady compression of the fluid. While a reduction of quantities (*I*) and (*II*) will clearly lead to a reduction sound power radiated by the small scale turbulence, modification of quantity (*III*) will engender both a change in the sound power as well as a spectral redistribution of the acoustic energy. It was seen in the aerodynamic results presented earlier how the Reynolds stresses are increased in the initial development region of the flow, increase characterised by high frequency scales, which could be expected to lead to a corresponding increase in the high frequency sound production. This is indeed found to be the case (figure 5). In the region downstream of $x/D = 2$, where characteristic space and time scales are larger, the global effect of the control is to reduce the Reynolds stresses, due to reduced mixing of the flow (here a link between the large and the small scale source mechanisms is evident, action on the former leading to reduction in the intensity of the latter). The expected effect would be a decrease in the lower frequency sound intensity. Again this is the trend observed.

The spatial correlation related to (ii) is a more complex quantity to analyse, comprising a 3 dimensional character which can only be partially obtained by a 2-D PIV measurement. Two components of the said tensor, R_{11} and R_{22} have nonetheless been estimated from the measurements - in order to give an indication of the kind of changes which the *fluidevrons* produce in this turbulence quantity. An example of these is shown in figure 3. In the case of the R_{11} term, not given here, there is little difference between the controlled and the un-controlled flow, aside from a slight modification of the correlation's orientation, related to the narrower shear layer in the controlled flow. On the other hand where the R_{22} component is concerned there is a substantial reduction in its spatial extent, again due to the decreased thickness of the shear layer. It is interesting to note that in Jordan *et al.* (2004) it was demonstrated how certain components of the sound production mechanisms would scale according to the square of the radial integral scale - small reductions in this quantity thus leading to significant reductions in the associated sound field. The global reduction of this quantity induced by the *fluidevrons* may therefore be of considerable importance. The difference is clear when we integrate these quantities over the 2D plane of the PIV measurement. The values obtained by this operation are shown in figure 12 as a function of axial position. While there is little change in the integral of the R_{11} term, for the R_{22} term the difference is clear, the controlled flow showing a considerably reduced correlation extent of its radial velocity component, up to 25% in the middle of the potential core region.

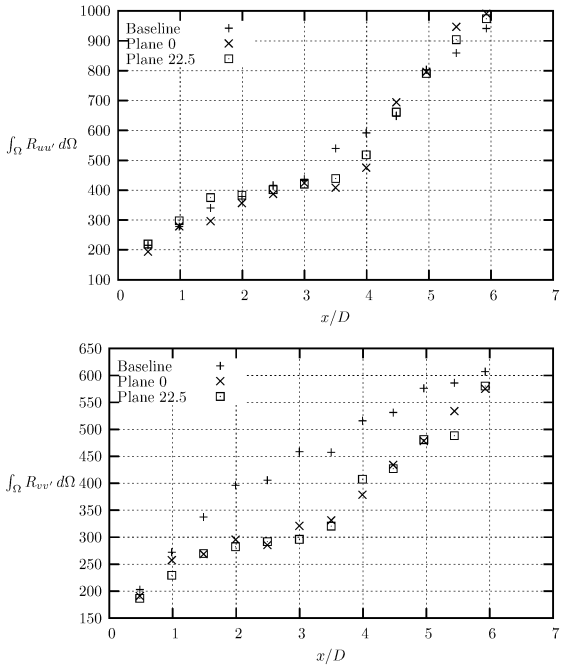

Figure 12: Longitudinal evolution of the spatial extent of correlations (arbitrary units)

As the PIV measurements can only give an indication of the spatial character of the flow, some preliminary hot-wire measurements were also performed, in order to understand the changes brought about in its temporal structure. An example is shown in figure 13, where an increase in the high frequency activity is observed near the exit plane. As discussed earlier this will result in high amplitude, high frequency sound production. Again this is the trend seen in the acoustic spectra. At further locations downstream, the spectra shows little difference in terms of frequency band.

CONCLUSIONS

A new jet noise control device, the *fluidevrons*, has been proposed based on the use of subscale jets to generate fluid deltas at the exit of a round jet. The aerodynamic and acoustic changes produced by this device have been studied. The acoustic effect is seen to be similar to that produced by the classical chevron, comprising a reduction of the sound intensity generated by the energy containing scales of the flow, a high

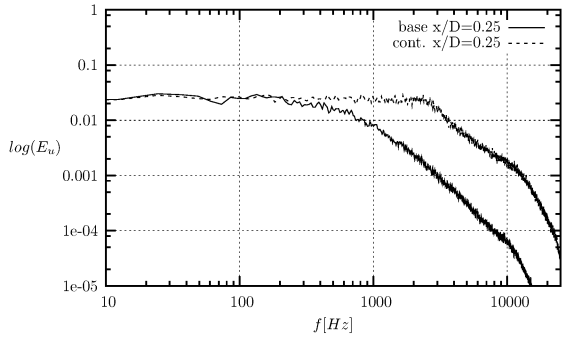

Figure 13: Effect on the u' spectrum, inside the jet mixing layer $x/D = 0.5$ and $y/D = 0.5$

frequency increase being the penalty paid. The cross-over frequency of the fluidevron is considerably higher however and the high frequency penalty less severe. This device has the added advantage that it can be turned off during cruise, thus avoiding drag penalty.

The aerodynamic character of the changes produced by the device have been studied in the context of the two sound production mechanisms considered important in the production of jet noise, the large coherent structures and the small scale turbulence. In both cases the aerodynamic effect of the *fluidevrons* is consistent with a reduced efficiency where both these mechanisms are concerned.

The principal effects are :

- Generation of longitudinal vorticity
- Disruption of the preferred azimuthal structure of the jet
- A subsequent reduction in mixing
- Reduced turbulence levels
- A longer potential core
- Reduced spatial extent of the radial velocity correlation

Further analysis will comprises two-point LDV measurements to obtain the time-scales, nearfield pressure measurements to be performed in a fully anechoic facility, and Proper Orthogonal Decompositions of both the velocity and the nearfield pressure fields with a view to better understanding the dynamic of the coherent structures.

Acknowledgements

The authors wish to thank Carine Fourment and Patrick Braud for their helpful part in the experiments.

REFERENCES

Bridges, J. and Brown, C.A. 2004, "Parametric testing of chevrons on single flow hot jets", *AIAA 10th Aeroacoustic conference* 2004-2824.

Bridges, J. and Wernet, M. "Turbulence measurements of separate flow nozzles with mixing enhancement features", *AIAA 8th Aeroacoustic conference* 2002-2484.

Callender, B. and Gutmark E. 2005, "A near-field investigation of chevron nozzle mechanisms", *AIAA 9th Aeroacoustic conference* 2003-3210.

Callender, B. and Gutmark E. 2005, "Far-field acoustic investigation into chevron nozzle mechanisms and trends", *AIAA Journal* vol.43, No.1. January 2005.

Christensen, K. T.,2004, "The influence of peak-locking errors on turbulence statistics computed from PIV ensembles", *Experiments in Fluids* vol.36, pp. 484-497.

GUJ, G. and al 2003, "Acoustic identification of coherent structures in a turbulent jet", *Journal of Sound and Vibration* vol.259, pp. 1037-1065.

Hileman, J. and al 2004, "Differences in dynamics of an ideally expanded Mach 1.3 jet during noise generation and relative quiet periods", *AIAA 10th Aeroacoustic conference* 2004-3015.

Jordan, P. and Gervais, Y. 2003, "Modelling self- and shear-noise mechanisms in inhomogeneous, anisotropic turbulence", *Journal od sound and vibration* vol 179, pp.529-55.

Jordan, P. and al 2004, "Acoustic-hydrodynamic interaction in the entrainment region of subsonic jet flow", *AIAA/CEAS 10th Aeroacoustic conference* 2004-3020.

Lighthill, M.J. 1952, "On sound generated aerodynamically", *Proceedings of the Royal Society* vol.211, pp 564-587.